Non-Hermitian mobility edges in one-dimensional quasicrystals with parity-time symmetry

Yanxia Liu,[1,*] Xiang-Ping Jiang,[1,2,*] Junpeng Cao,[1,2,3] and Shu Chen[1,2,4,†]

[1]*Beijing National Laboratory for Condensed Matter Physics, Institute of Physics, Chinese Academy of Sciences, Beijing 100190, China*

[2]*School of Physical Sciences, University of Chinese Academy of Sciences, Beijing 100049, China*

[3]*Songshan Lake Materials Laboratory, Dongguan, Guangdong 523808, China*

[4]*Yangtze River Delta Physics Research Center, Liyang, Jiangsu 213300, China*

(Received 19 February 2020; accepted 5 May 2020; published 21 May 2020)

We investigate the localization-delocalization transition in one-dimensional non-Hermitian quasiperiodic lattices with exponential short-range hopping, which possess parity-time ($\mathcal{PT}$) symmetry. The localization transition induced by the non-Hermitian quasiperiodic potential is found to occur at the $\mathcal{PT}$-symmetry-breaking point. Our results also demonstrate the existence of energy-dependent mobility edges, which separate the extended states from localized states and are only associated with the real part of eigenenergies. The level statistics and Loschmidt echo dynamics are also studied.

DOI: 10.1103/PhysRevB.101.174205

I. INTRODUCTION

Ever since the seminal work of Anderson [1], Anderson localization has become a fundamental paradigm for the study of localization induced by random disorder in condensed-matter physics. While all eigenstates are localized in the presence of infinitesimal disorder strengths in one- and two-dimensional noninteracting systems, localized and extended states can coexist at different energies in three dimensions with a single-particle mobility edge (SPME) [2–4], i.e., a critical energy separating localized and delocalized energy eigenstates. As an intermediate case between the disordered and periodic systems, quasicrystals display very different behaviors and may support a localization-delocalization transition even in one dimension. A well-known example is given by a one-dimensional (1D) quasiperiodic system described by the Aubry-André (AA) model [5,6], which undergoes a localization transition when the strength of the quasiperiodical potential exceeds a critical point determined by the self-duality condition. The AA model has been experimentally realized in bichromatic optical lattices [7–11]. By introducing short-range or long-range hopping processes, some modified AA models may support energy-dependent mobility edges [12–18], which were found to appear in other quasiperiodic models [19–25]. Experimental observation of mobility edge and many-body localization in 1D quasiperiodic optical lattices was also reported in recent works [26,27].

Recently, there has been growing interest in non-Hermitian Hamiltonians from theory to experiment [28–35]. In general, the non-Hermiticity is achieved by introducing nonreciprocal hopping processes or gain and loss terms, which may induce exotic phenomena without Hermitian counterparts, such as parity-time ($\mathcal{PT}$) phase transitions [28,36–38], non-Hermitian skin effect [39–53], and exceptional points [54,55]. The dynamics associated with exception points in non-Hermitian systems exhibits a lot of unexpected and interesting results, such as the realization of dynamical encircling of exceptional points [56,57], enhanced sensing for application [58,59], and so on. The interplay of non-Hermiticity and disorder was studied in terms of the Hatano-Nelson-type models [60–64], in which the nonreciprocal hopping introduced in the 1D Anderson model leads to a finite localization-delocalization transition. and non-Hermitian Anderson models with complex on-site disorder potentials [65,66]. The effects of non-Hermiticity on quasiperiodic lattices have been studied in different contexts [67–73]. However, the non-Hermitian effect on the mobility edges in quasicrystals is still lacking. Since the eigenvalues of a non-Hermitian system are generally complex, particularly interesting questions arise here: Are there any existing mobility edges in the non-Hermitian quasiperiodic lattices with short-range or long-range hopping? If so, how do we characterize the non-Hermitian mobility edge?

In this work, we address these questions by studying a non-Hermitian extension of the AA model with exponentially decaying short-range hopping and $\mathcal{PT}$ symmetry. By analyzing the spatial distribution of wave functions and spectral information, we find that the increase of quasiperiodic potential strength can lead a localization transition at the $\mathcal{PT}$-symmetry breaking point, and unveil that there exists an intermediate regime with mobility edges, which separate the extended states from localized states and are only relevant to the real part of the spectrum. We also analyze the level statistics and study the Loschmidt echo dynamics of the system.

II. GENERALIZED NON-HERMITIAN AA MODEL

We consider a 1D tight-binding model with short-range hopping terms and a non-Hermitian quasiperiodic potential, described by

$$Eu_n = \sum_{n' \neq n} t e^{-p|n-n'|} u_{n'} + V_n u_n, \tag{1}$$

*These authors contributed equally to this work.

†Corresponding author: schen@iphy.ac.cn

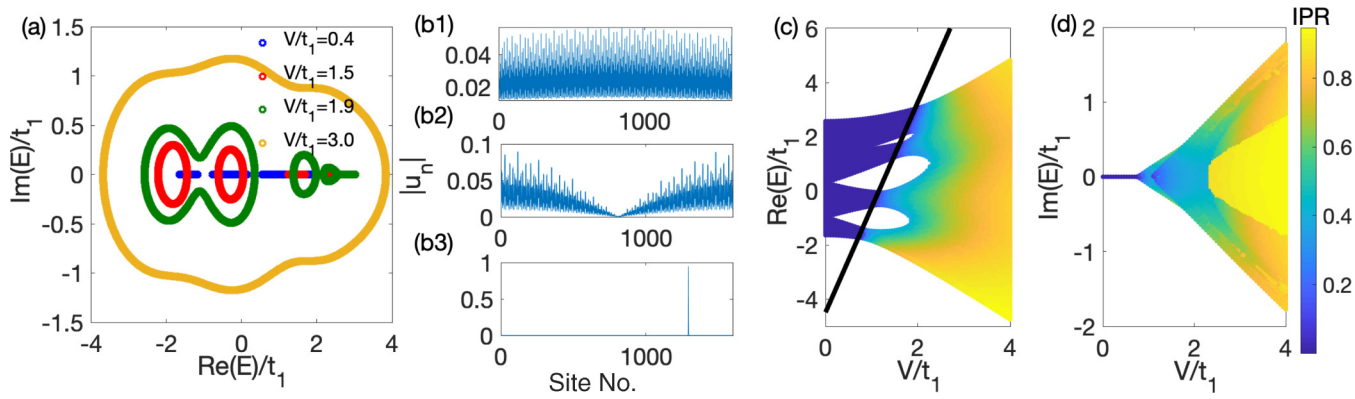

FIG. 1. Energy eigenvalues and eigenstates of Eq. (1) with lattice sites $L = 1597$, $\alpha = (\sqrt{5}-1)/2$, $p = 1.5$, and $h = 0.5$ under PBC. (a) The complex eigenenergies for systems with $V/t_1 = 0.4$, 1.5, 1.9, and 3.0. Distributions of eigenstates corresponding to different eigenvalues for the system with $V/t_1 = 1.9$: (b1) $\mathrm{Re}(E) > \mathrm{Re}(E_c)$ and the corresponding state is an extended state above the mobility edge, (b2) $\mathrm{Re}(E) \approx \mathrm{Re}(E_c)$ and the state is a critical state near the mobility edge, (b3) $\mathrm{Re}(E) < \mathrm{Re}(E_c)$ and the state is a localized state below the mobility edge. (c) The shading of real energy curves indicates the magnitude of the IPR for the corresponding eigenstates, and the black solid line represents the boundary given by Eq. (6), which separates the localized and extended states. (d) The corresponding imaginary energies of (c).

where t is the hopping amplitude with the exponentially decaying parameter $p > 0$ and the on-site potential V_n is given by

$$V_n = V\cos(2\pi\alpha n + \phi). \tag{2}$$

Here, V is the potential strength, α is an irrational number, and $\phi = \theta + ih$ describes a complex phase factor. When $h = 0$, the model reduces to the Hermitian model studied in Refs. [12,13], which is an exponential hopping generalization of the AA model. The AA model only includes a nearest-neighbor hopping term with the hopping amplitude

$$t_1 = te^{-p}, \tag{3}$$

and manifests a localization-delocalization transition for all eigenstates at the self-dual point $V = 2t_1$. For a finite $p > 0$, the generalized AA model has energy-dependent mobility edges given by $\cosh(p) = \frac{E+t}{V}$, which was determined by a generalized self-dual transformation [12,13]. We note that the transition point and mobility edges are independent of the value of phase factor θ in the Hermitian limit.

Now we consider the non-Hermitian case with $h \neq 0$. Particularly, we shall consider the case with $\theta = 0$, for which we have $V_n = V_{-n}^*$ and the non-Hermitian model fulfills $\mathcal{PT}$ symmetry. In the following, we shall study the $\mathcal{PT}$-symmetric generalized AA (GAA) model with

$$V_n = V\cos(2\pi\alpha n + ih), \tag{4}$$

and take $\alpha = (\sqrt{5}-1)/2$ in the whole paper. We note that similar physics is found for α taking other values of irrational numbers. Due to the existence of $\mathcal{PT}$ symmetry, one may expect that all eigenvalues of the GAA model are real if the $\mathcal{PT}$ symmetry is unbroken. In Fig. 1(a), we display all the eigenvalues of the system with $p = 1.5$, $h = 0.5$ and various V in the complex space of energies. For convenience, here we take t_1 as the unit of energy, and the periodic boundary condition (PBC) is considered. It is shown that all the eigenvalues are real when $V/t_1 = 0.4$. Further increasing the potential strength V and exceeding a certain threshold $V_{c_1}/t_1 = 0.702$, the eigenvalues with $\mathrm{Re}(E)$ below a critical value E_c become complex accompanying the breakdown of $\mathcal{PT}$ symmetry, whereas above a critical value E_c, they remain real, as shown in Fig. 1(a) for $V/t_1 = 1.5$ and 1.9. When V exceeds the second threshold, $V_{c_2}/t_1 = 2.02$, all eigenvalues are complex, as shown in Fig. 1(a) for $V/t_1 = 3$.

By inspecting the spatial distribution of the eigenstates, we find that all the states with complex eigenvalues are localized states, whereas the states with real eigenvalues are extended states distributing over the whole lattice. This suggests that the localization transition is simultaneously accompanied by the $\mathcal{PT}$-symmetry-breaking transition. In Fig. 1(b), we display the distributions of wave functions with the real part of eigenvalues $\mathrm{Re}(E)$ above, close to, and below the critical value $\mathrm{Re}(E_c)$ for the system with $V/t_1 = 1.9$. It is clear that the state with $\mathrm{Re}(E)$ above the critical value is an extended state and the state below the critical value is a localized state. This clearly indicates that there exists a regime where the localized and extended states coexist and are separated by mobility edges, when V is in the region $V_{c_1} < V < V_{c_2}$.

Next we determine the mobility edges numerically. In order to characterize the localization properties of an eigenstate, we calculate the inverse participation ratio (IPR) defined as

$$\mathrm{IPR}^{(i)} = \frac{\sum_n |u_n^i|^4}{\left(\sum_n |u_n^i|^2\right)^2}, \tag{5}$$

where the superscript i denotes the ith eigenstate of the system, and n labels the lattice coordinate. Here the corresponding complex energy E_i is indexed according to their real part $\mathrm{Re}(E_i)$ in ascending order. For a full localized eigenstate, the IPR is finite and $\mathrm{IPR} \simeq 1$. For an extended state, the $\mathrm{IPR} \simeq 1/L$ and approaches zero when L tends to infinity. In Figs. 1(c) and 1(d), we plot the real parts and imaginary parts of the eigenvalues as well as the IPR of the corresponding wave functions versus the potential strength V, respectively. The black solid line in Fig. 1(c) marks the transition points, which separate the extended and localized states, with the

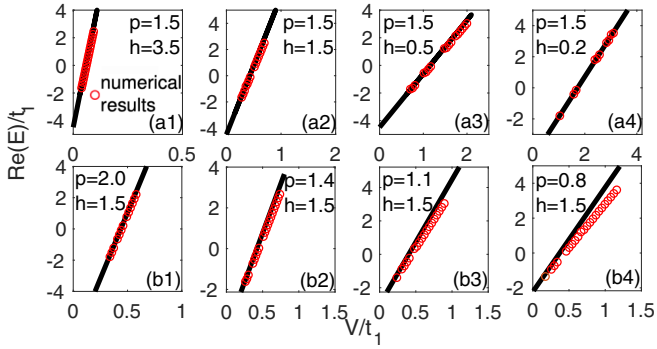

FIG. 2. Numerical results of mobility edges obtained from IPRs and spectrum (red circles) for systems with $L = 1597$ and different parameters (a1)–(a4) $p = 1.5$ and $h = 3.5$, 1.5, 0.5, and 0.2, and (b1)–(b4) $h = 1.5$ and $p = 2.0$, 1.4, 1.1 and 0.8, respectively. The black solid lines are obtained using Eq. (6).

values of IPR above which approach zero and below which are finite. Such a line gives the mobility edge and is found to be well described by a simple relation,

$$\cosh(p) = \frac{\mathrm{Re}(E) + t}{Ve^{|h|}}. \tag{6}$$

Despite a lack of exact proof, the above analytical relation for the mobility edge boundary agrees well with the numerical results from IPR and spectrum calculations. As shown in Figs. 2(a1)–2(a4), the numerical results of the mobility edges for systems with $p = 1.5$ and various h are well described by Eq. (6). In Figs. 2(b1)–2(b4), we display the numerical results for systems with fixed $h = 1.5$ and various p. It is shown that Eq. (6) agrees with the numerical results for systems with $p = 2.5$ and 1.4, and deviation can be observed for $p = 1.1$. From our numerical results, we find that Eq. (6) fails to describe SPMEs of systems with $p < 1$ [see Fig. 2(b4)]. When p is small, the effect of long-range hopping becomes more important. Although these systems still support mobility edges, we are not able to get a simple analytical expression for them. We have become aware of the existence of mobility edges in the non-Hermitian GAA model. To distinguish the region with SPMEs from the extended and localized regions, it is convenient to consider the normalized participation ratio (NPR) defined as [15–17],

$$\mathrm{NPR}^{(i)} = \left[L \sum_n \left| u_n^i \right|^4 \right]^{-1}, \tag{7}$$

which is a complementary quantity for the IPR. Taking the average over all eigenstates, we can get the averaged NPR ($\langle \mathrm{NPR} \rangle$) and IPR ($\langle \mathrm{IPR} \rangle$), which provide complete complementary information for the extended, intermediate, and localized phases. We calculate the NPR and IPR for all eigenstates of the non-Hermitian GAA model and display their average values in Fig. 3(a), which clearly shows the existence of three distinct phases depending on the strength of the quasiperiodic potential V/t_1 for the given parameters $p = 1.5$ and $h = 0.5$. When the potential strength is smaller than the threshold $V_{c_1}/t_1 = 0.702$, all eigenstates are extended, as indicated by a vanishing $\langle \mathrm{IPR} \rangle$ and a finite $\langle \mathrm{NPR} \rangle$. When the potential strength exceeds the second threshold $V_{c_2}/t_1 = 2.02$, all eigenstates are localized, as indicated by a finite $\langle \mathrm{IPR} \rangle$ and a vanishing $\langle \mathrm{NPR} \rangle$. When the potential strength lies in between two thresholds, an intermediate regime with both finite $\langle \mathrm{IPR} \rangle$ and $\langle \mathrm{NPR} \rangle$ is characterized by the coexistence of extended and localized states, which can also be read out from the distribution of IPRs for all eigenstates, as shown in Fig. 3(b).

We display the average IPR in the two-dimensional parameter space V/t_1 versus h in Fig. 3(c), in which the blue solid lines distinguish the extended, intermediate, and localized regime, respectively. When gradually increasing h, the intermediate regime with SPME diminishes. On the other hand, if we fix h and increase p, the intermediate regime with SPME also diminishes. Particularly, when $p \to \infty$, our model reduces to the non-Hermitian AA model with only nearest-neighboring hopping [69,70], and Eq. (6) reduces to

$$Ve^{|h|} = 2t_1, \tag{8}$$

indicating the absence of a mobility edge.

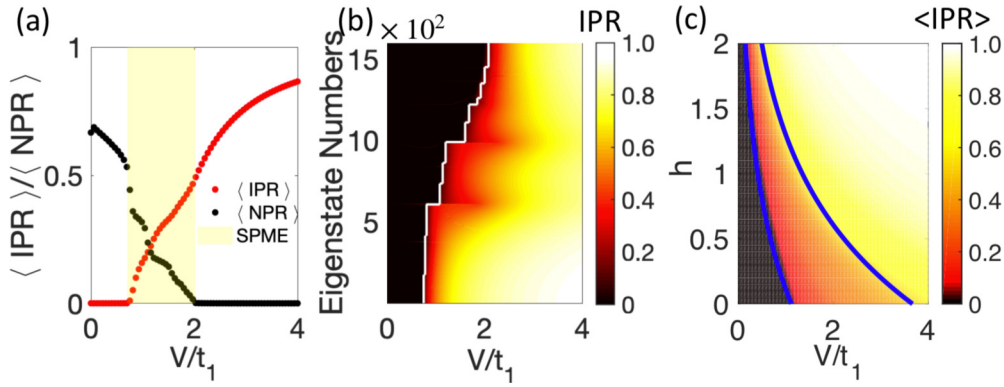

FIG. 3. Mobility edges for the non-Hermitian GAA model with lattice sites $L = 1597$, $\alpha = (\sqrt{5} - 1)/2$, and $p = 1.5$. (a) Averaged IPR and NPR for all eigenstates in our lattice model with $h = 0.5$. (b) IPR of all eigenstates for the system with $h = 0.5$. Here, eigenstates numbers are ordered by $\mathrm{Re}(E)$. The white lines mark out the SPME. (c) Phase diagram in the parameter space spanned by V/t_1 and h. The blue solid lines are the phase boundaries separated by the intermediate regime from the extended and localized regimes, which can be obtained numerically using Eq. (6).

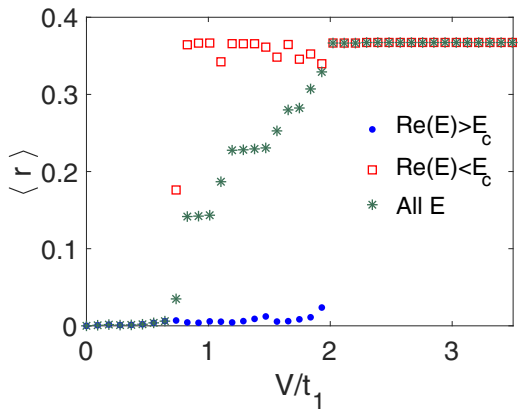

FIG. 4. The average of the adjacent gap ratio $\langle r\rangle$ for systems with $L = 1597$, $\alpha = (\sqrt{5}-1)/2$, $p = 1.5$, $h = 0.5$ and different V vs V/t_1.

III. LEVEL STATISTICS AND LOSCHMIDT-ECHO DYNAMICS

The level statistics provides a powerful tool to characterize the localization transition in Hermitian disorder systems [15,74–79]. For our non-Hermitian model, the eigenvalues in the localized regime are complex. The nearest-neighboring level spacing statistics for non-Hermitian disorder systems has been investigated in terms of non-Hermitian random-matrix theory [80–83]. According to Eq. (6), the mobility edge is only associated with the real part of the complex energies, and it is reasonable to count the real part of level spacings. So, we calculate the adjacent gap ratio r of ordering $\mathrm{Re}(E)$, which is given as

$$r_n = \frac{\min(s_n, s_{n-1})}{\max(s_n, s_{n-1})}, \tag{9}$$

with s_n the level spacing between the real part of the nth and $(n-1)$-th eigenenergies. The average of r_n is introduced as

$$\langle r\rangle = \frac{1}{L}\sum_n r_n. \tag{10}$$

In Fig. 4, we show the real level statistics across the localization transition. The average value $\langle r\rangle$ approaches zero in the delocalized phase, whereas it approaches 0.386 in the localized phase, which is identical to the expected value from Poisson statistics as in the Hermitian disorder systems. For the intermediate regime with mobility edges, the value $\langle r\rangle$ presents a steplike growth from zero to 0.386. This is consistent with the result shown in Fig. 3(a). In the intermediate regime, if we count the level statistics for the states above or below the mobility edges separately, the average value $\langle r\rangle$ approaches the value in the extended or localized regime, respectively, as shown in Fig. 4.

The Loschmidt echo is an important quantity for describing quench dynamics [84–88], which measures the overlap of an initial quantum state and its time-evolution state after a quench process. The behavior of the Loschmidt echo is related to both the initial state and postquench states. It was shown that the Loschmidt-echo dynamics can characterize the localization-delocalization transition in a standard AA model [89], and was applied to study the dynamical observation of mobility edges in 1D incommensurate optical lattices [90]. The exotic dynamical phenomenon in some other $\mathcal{PT}$-symmetric systems has also been studied [91,92]. Here, we explore the Loschmidt-echo characteristic of our non-Hermitian quasiperiodic system. The system is initially prepared in the eigenstate $|\phi_i\rangle$ of an initial Hamiltonian H_i with tunable parameter $V = V_i$. Then the potential strength is suddenly switched to a new value V_f, resulting in a final state

$$|\phi_f(t)\rangle = e^{-itH_f}|\phi_i\rangle, \tag{11}$$

where e^{-itH_f} is the evolution operator after quenching and $\hbar = 1$ is set for convenience. We need to emphasize that for the final system with real eigenvalues, the final state oscillates over time, and for the final system with complex eigenvalues, the final state becomes a steady state for a long time, which is similar to the imaginary-time evolution for finding the ground state of a Hermitian system. The difference is that for the non-Hermitian system, the steady state is an eigenstate of the final system with the maximum eigenvalue of the imaginary part, instead of the ground state. The form of the Loschmidt echo is

$$L(t) = \frac{|\langle\phi_i|\phi_f(t)\rangle|^2}{\langle\phi_i|\phi_i\rangle\langle\phi_f(t)|\phi_f(t)\rangle}, \tag{12}$$

where the denominator is introduced to make sure that the initial and final states are normalized. The dynamics of the non-Hermitian system is a kind of nonunitary dynamics, due to the existence of complex eigenvalues.

Figures 5(a) and 5(e) show the quench dynamics for initial states prepared as eigenstates of the system in the extended regime with $V_i = 0.2$, corresponding to minimum and maximum eigenvalues, respectively. For the final systems with $V_f = 0.4$ and $V_f = 0.7$, they locate in the same regime as the initial system with all eigenvalues being real, and $L(t)$ oscillates with a positive lower bound, which never approaches zero during the evolution process. When the final system locates in the mixed regime with $V_f = 1.5$ and $V_f = 2.0$, respectively, both the real and complex eigenvalues coexist, and $L(t)$ oscillates at short time but approaches zero at long times. When the final system is in the localized regime with $V_f = 2.5$, $L(t)$ exhibits similar behavior as in the mixing regime.

Figures 5(b) and 5(f) show the quench dynamics for initial states prepared in the mixing regime with $V_i = 1.4$, corresponding to the minimum and maximum of the real part of the eigenvalues, respectively. As one of the initial states is a localized state and another is an extended state, they exhibit different dynamical behaviors. While the latter one is similar to the case shown Fig. 5(e), the former one is similar to cases with the initial state prepared in the localized regime with $V_i = 2.7$, as shown in Figs. 5(c) and 5(g), where $L(t)$ always approaches zero at long times for the final systems in different regimes. Our results demonstrate that the Loschmidt echo exhibits different dynamical behaviors for systems with initial states in different regimes.

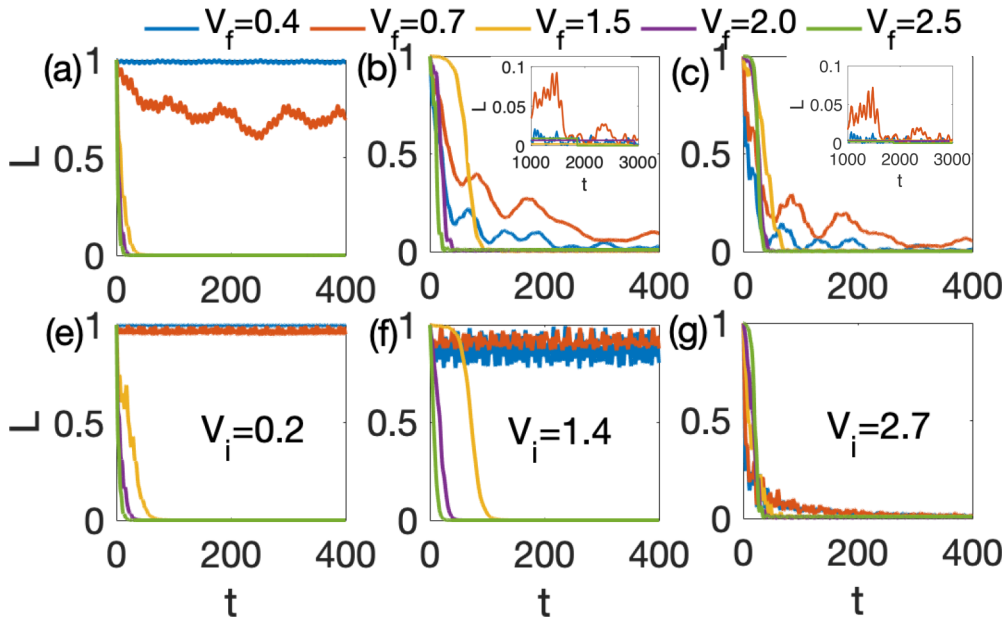

FIG. 5. Evolution of Loschmidt echo. The initial state is chosen to be the state corresponding to the minimum and maximum of the real part of the eigenvalues of the initial Hamiltonian with (a), (e) $V_i = 0.2$, (b), (f) $V_i = 1.4$, (c), (g) $V_i = 2.7$, respectively. Different V_f are shown by different colors. Here we have set the energy unit $t_1 = 1$.

IV. SUMMARY

In summary, we studied the localization transition induced by a non-Hermitian quasiperiodic potential in 1D $\mathcal{PT}$-symmetric quasicrystals, described by the non-Hermitian GAA model with exponential hopping. Our results demonstrate that there exist three different regimes, i.e., extended, mixed, and localized phases. While all the eigenstates are either extended or localized in the extended or localized regime, the extended and localized states coexist in the mixed regime and are separated by energy-dependent mobility edges. By analyzing the distribution of wave functions and the corresponding eigenenergies, we found that the localization transition is always accompanied by the $\mathcal{PT}$-symmetry-breaking transition and the mobility edges only depend on the real part of the energies. We also investigated the level statistics and Loschmidt-echo dynamics in our non-Hermitian quasiperiodic systems and unveiled that they display different behaviors in different regimes.

ACKNOWLEDGMENTS

We thank Y. C. Wang for helpful discussions. The work is supported by NSFC under Grant No. 11974413 and the National Key Research and Development Program of China (Grants No. 2016YFA0300600 and No. 2016YFA0302104).

[1] P. W. Anderson, Absence of diffusion in certain random lattices, Phys. Rev. **109**, 1492 (1958).

[2] E. Abrahams, P. W. Anderson, D. C. Licciardello, and T. V. Ramakrishnan, Scaling Theory of Localization: Absence of Quantum Diffusion in Two Dimensions, Phys. Rev. Lett. **42**, 673 (1979).

[3] P. A. Lee and T. V. Ramakrishnan, Disordered electronic systems, Rev. Mod. Phys. **57**, 287 (1985).

[4] F. Evers and A. D. Mirlin, Anderson transitions, Rev. Mod. Phys. **80**, 1355 (2008).

[5] S. Aubry and G. André, Analyticity breaking and anderson localization in incommensurate lattices, Ann. Israel Phys. Soc. **3**, 133 (1980).

[6] P. G. Harper, Single band motion of conduction electrons in a uniform magnetic field, Proc. Phys. Soc. A **68**, 874 (1955).

[7] G. Roati, C. DErrico, L. Fallani, M. Fattori, C. Fort, M. Zaccanti, G. Modugno, M. Modugno, and M. Inguscio, Anderson localization of a non-interacting Bose-Einstein condensate, Nature (London) **453**, 895 (2008).

[8] J. Billy, V. Josse, Z. C. Zuo, A. Bernard, B. Hambrecht, P. Lugan, D. Clément, L. Sanchez-Palencia, P. Bouyer, and A. Aspect, Direct observation of Anderson localization of matter waves in a controlled disorder, Nature (London) **453**, 891 (2008).

[9] F. Jendrzejewski, A. Bernard, K. Mueller, P. Cheinet, V. Josse, M. Piraud, L. Pezzé, L. Sanchez-Palencia, A. Aspect, and P. Bouyer, Three-dimensional localization of ultracold atoms in an optical disordered potential, Nat. Phys. **8**, 398 (2012).

[10] W. R. McGehee, S. S. Kondov, W. Xu, J. J. Zirbel, and B. DeMarco, Three-Dimensional Anderson Localization in Variable Scale Disorder, Phys. Rev. Lett. **111**, 145303 (2013).

[11] S. S. Kondov, W. R. McGehee, J. J. Zirbel, and B. DeMarco, Three-dimensional Anderson localization of ultracold matter, Science **334**, 66 (2011).

[12] J. Biddle, D. J. Priour, B. Wang, and S. Das Sarma, Localization in one-dimensional lattices with non-nearest-neighbor hopping: Generalized Anderson and Aubry- André models, Phys. Rev. B **83**, 075105 (2011).

[13] J. Biddle and S. Das Sarma, Predicted Mobility Edges in One-Dimensional Incommensurate Optical Lattices: An Exactly Solvable Model of Anderson Localization, Phys. Rev. Lett. **104**, 070601 (2010).

[14] S. Ganeshan, J. H. Pixley, and S. Das Sarma, Nearest Neighbor Tight Binding Models with an Exact Mobility Edge in One Dimension, Phys. Rev. Lett. **114**, 146601 (2015).

[15] X. P. Li, J. H. Pixley, D. L. Deng, S. Ganeshan, and S. Das Sarma, Quantum nonergodicity and fermion localization in a system with a single-particle mobility edge, Phys. Rev. B **93**, 184204 (2016).

[16] X. Li, X. P. Li, and S. Das Sarma, Mobility edges in one-dimensional bichromatic incommensurate potentials, Phys. Rev. B **96**, 085119 (2017).

[17] X. Li and S. Das Sarma, Mobility edge and intermediate phase in one-dimensional incommensurate lattice potentials, Phys. Rev. B **101**, 064203 (2020).

[18] X. Deng, S. Ray, S. Sinha, G. V. Shlyapnikov, and L. Santos, One-Dimensional Quasicrystals with Power-Law Hopping, Phys. Rev. Lett. **123**, 025301 (2019).

[19] S. Das Sarma, S. He, and X. C. Xie, Mobility Edge in a Model One-Dimensional Potential, Phys. Rev. Lett. **61**, 2144 (1988).

[20] D. J. Thouless, Localization by a Potential with Slowly Varying Period, Phys. Rev. Lett. **61**, 2141 (1988).

[21] S. Das Sarma, S. He, and X. C. Xie, Localization, mobility edges, and metal-insulator transition in a class of one-dimensional slowly varying deterministic potentials, Phys. Rev. B **41**, 5544 (1990).

[22] D. J. Boers, B. Goedeke, and D. Hinrichs, M. Holthaus, Mobility edges in bichromatic optical lattices, Phys. Rev. A **75**, 063404 (2007).

[23] A. M. Guo, X. C. Xie, and Q.-F. Sun, Delocalization and scaling properties of low-dimensional quasiperiodic systems, Phys. Rev. B **89**, 075434 (2014).

[24] M. Rossignolo and L. Dell'Anna, Localization transitions and mobility edges in coupled Aubry-Andre chains, Phys. Rev. B **99**, 054211 (2019).

[25] F. A. An, E. J. Meier, and B. Gadway, Engineering a Flux-Dependent Mobility Edge in Disordered Zigzag Chains, Phys. Rev. X **8**, 031045 (2018).

[26] H. P. Lüschen, S. Scherg, T. Kohlert, M. Schreiber, P. Bordia, X. Li, S. Das Sarma, and I. Bloch, Single-Particle Mobility Edge in a One-Dimensional Quasiperiodic Optical Lattice, Phys. Rev. Lett. **120**, 160404 (2018).

[27] T. Kohlert, S. Scherg, X. Li, H. P. Lüschen, S. Das Sarma, I. Bloch, and M. Aidelsburger, Observation of Many-Body Localization in a One-Dimensional System with a Single-Particle Mobility Edge, Phys. Rev. Lett. **122**, 170403 (2019).

[28] C. M. Bender and S. Boettcher, Real Spectra in Non-Hermitian Hamiltonians Having $\mathcal{PT}$ Symmetry, Phys. Rev. Lett. **80**, 5243 (1998).

[29] T. Ozawa, H. M. Price, A. Amo, N. Goldman, M. Hafezi, L. Lu, M. Rechtsman, D. Schuster, J. Simon, O. Zilberberg, and I. Carusotto, Topological photonics, Rev. Mod. Phys. **91**, 015006 (2019).

[30] A. Guo, G. J. Salamo, D. Duchesne, R. Morandotti, M. Volatier-Ravat, V. Aimez, G. A. Siviloglou, and D. N. Christodoulides, Observation of PT -Symmetry Breaking in Complex Optical Potentials, Phys. Rev. Lett. **103**, 093902 (2009).

[31] Z. Gong, Y. Ashida, K. Kawabata, K. Takasan, S. Higashikawa, and M. Ueda, Topological Phases of Non-Hermitian Systems, Phys. Rev. X **8**, 031079 (2018).

[32] C. Liu, H. Jiang, and S. Chen, Topological classification of non-Hermitian systems with reflection symmetry, Phys. Rev. B **99**, 125103 (2019).

[33] K. Kawabata, K. Shiozaki, M. Ueda, and M. Sato, Symmetry and Topology in Non-Hermitian Physics, Phys. Rev. X **9**, 041015 (2019).

[34] H. Zhou and J. Y. Lee, Periodic table for topological bands with non-Hermitian symmetries, Phys. Rev. B **99**, 235112 (2019).

[35] C. Liu and S. Chen, Topological classification of defects in non-Hermitian systems, Phys. Rev. B **100**, 144106 (2019).

[36] K. Esaki, M. Sato, K. Hasebe, and M. Kohmoto, Edge states and topological phases in non-Hermitian systems, Phys. Rev. B **84**, 205128 (2011).

[37] B. Zhu, R. Lü, and S. Chen, PT symmetry in the non-Hermitian Su-Schrieffer-Heeger model with complex boundary potentials, Phys. Rev. A **89**, 062102 (2014).

[38] C. Yuce, Topological phase in a non-Hermitian PT symmetric system, Phys. Lett. A **379**, 1213 (2015).

[39] T. E. Lee, Anomalous Edge State in a Non-Hermitian Lattice, Phys. Rev. Lett. **116**, 133903 (2016).

[40] D. Leykam, K. Y. Bliokh, C. Huang, Y. D. Chong, and F. Nori, Edge Modes, Degeneracies, and Topological Numbers in Non-Hermitian Systems, Phys. Rev. Lett. **118**, 040401 (2017).

[41] H. Shen, B. Zhen, and L. Fu, Topological Band Theory For Non-Hermitian Hamiltonians, Phys. Rev. Lett. **120**, 146402 (2018).

[42] C. Yin, H. Jiang, L. Li, R. Lü and S. Chen, Geometrical meaning of winding number and its characterization of topological phases in one-dimensional chiral non-Hermitian systems, Phys. Rev. A **97**, 052115 (2018).

[43] S. Lieu, Topological phases in the non-Hermitian Su-Schrieffer-Heeger model, Phys. Rev. B **97**, 045106 (2018).

[44] S. Yao and Z. Wang, Edge States and Topological Invariants of Non-Hermitian Systems, Phys. Rev. Lett. **121**, 086803 (2018).

[45] V. M. Martinez Alvarez, J. E. Barrios Vargas, and L. E. F. Foa Torres, Non-Hermitian robust edge states in one dimension: Anomalous localization and eigenspace condensation at exceptional points, Phys. Rev. B **97**, 121401(R) (2018).

[46] Y. Xiong, Why does bulk boundary correspondence fail in some non-Hermitian topological models, J. Phys. Commun. **2**, 035043 (2018).

[47] F. K. Kunst, E. Edvardsson, J. C. Budich, and E. J. Bergholtz, Biorthogonal, Bulk-Boundary Correspondence in Non-Hermitian Systems, Phys. Rev. Lett. **121**, 026808 (2018).

[48] S. Yao, F. Song, and Z. Wang, Non-Hermitian Chern Bands, Phys. Rev. Lett. **121**, 136802 (2018).

[49] C. H. Lee and R. Thomale, Anatomy of skin modes and topology in non-hermitian systems, Phys. Rev. B **99**, 201103 (2019).

[50] D. S. Borgnia, A. J. Kruchkov, R.-J. Slager, Non-Hermitian Boundary Modes, Phys. Rev. Lett. **124**, 056802 (2020).

[51] K. Yokomizo and S. Murakami, Non-Bloch Band Theory of Non-Hermitian System, Phys. Rev. Lett. **123**, 066404 (2019).

[52] K. Zhang, Z. Yang, and C. Fang, Correspondence between winding numbers and skin modes in non-Hermitian systems, arXiv:1910.01131.

[53] N. Okuma, K. Kawabata, K. Shiozaki, and M. Sato, Topological Origin of Non-Hermitian Skin Effects, Phys. Rev. Lett. **124**, 086801 (2020).
[54] A. Mostafazadeh, Psedo-Hermitian representation of quantum mechanics, Int. J. Geom. Meth. Mod. Phys. **7**, 1191 (2010).
[55] M. Znojil, Unitarity corridors to exceptional points, Phys. Rev. A **100**, 032124 (2019).
[56] T. J. Milburn, J. Doppler, Catherine A. Holmes, S. Portolan, S. Rotter, and P. Rabl, General description of quasiadiabatic dynamical phenomena near exceptional points, Phys. Rev. A **92**, 052124 (2015).
[57] J. Doppler, A. A. Mailybaev, J. Böhm, U. Kuhl, A. Girschik, F. Libisch, T. J. Milburn, P. Rabl, N. Moiseyev, and S. Rotter, Dynamically Encircling an Exceptional Point for Asymmetric Mode Switching, Nature (London) **537**, 76 (2016).
[58] W. Chen, S. K. Özdemir, G. Zhao, J. Wiersig, and L. Yang, Exceptional Points Enhance Sensing in an Optical Microcavity, Nature (London) **548**, 192 (2017).
[59] L. Pan, S. Chen, and X. Cui, High-order exceptional points in ultracold Bose gases, Phys. Rev. A **99**, 011601(R) (2019).
[60] N. Hatano and D. R. Nelson, Localization Transitions in Non-Hermitian Quantum Mechanics, Phys. Rev. Lett. **77**, 570 (1996).
[61] N. Hatano and D. R. Nelson, Non-Hermitian delocalization and eigenfunctions, Phys. Rev. B **58**, 8384 (1998).
[62] N. M. Shnerb and D. R. Nelson, Winding Numbers, Complex Currents, and Non-Hermitian Localization, Phys. Rev. Lett. **80**, 5172 (1998).
[63] J. Feinberg and A. Zee, Non-Hermitian localization and delocalization, Phys. Rev. E **59**, 6433 (1999).
[64] A. V. Kolesnikov and K. B. Efetov, Localization- Delocalization Transition in Non-Hermitian Disordered Systems, Phys. Rev. Lett. **84**, 5600 (2000).
[65] A. F. Tzortzakakis, K. G. Makris, and E. N. Economou, Non-Hermitian disorder in two-dimensional optical lattices, Phys. Rev. B **101**, 014202 (2020).
[66] Y. Huang and B. I. Shklovskii, Anderson transition in three-dimensional systems with non-Hermitian disorder, Phys. Rev. B **101**, 014204 (2020).
[67] A. Jazaeri and I. I. Satija, Localization transition in incommensurate non-Hermitian systems, Phys. Rev. E **63**, 036222 (2001).
[68] Q.-B. Zeng, S. Chen, and R. Lu, Anderson localization in the non-Hermitian Aubry-Andre-Harper model with physical gain and loss, Phys. Rev. A **95**, 062118 (2017).
[69] S. Longhi, Topological Phase Transition in Non-Hermitian Quasicrystals, Phys. Rev. Lett. **122**, 237601 (2019).
[70] H. Jiang, L. J. Lang, C. Yang, S. L. Zhu, and S. Chen, Interplay of non-Hermitian skin effects and Anderson localization in nonreciprocal quasiperiodic lattices, Phys. Rev. B **100**, 054301 (2019).
[71] Q. B. Zeng, Y. B. Yang, and Y. Xu, Topological phases in non-Hermitian Aubry-André-Harper models, Phys. Rev. B **101**, 020201 (2020).
[72] S. Longhi, Metal-insulator phase transition in a non-Hermitian Aubry-André-Harper model, Phys. Rev. B **100**, 125157 (2019).
[73] R. Wang, K. L. Zhang, and Z. Song, Anderson localization induced by complex potential, arXiv:1909.12505.
[74] S. N. Evangelou and E. N. Economou, Spectral Density Singularities, Level Statistics, and Localization in a Sparse Random Matrix Ensemble, Phys. Rev. Lett. **68**, 361 (1992).
[75] B. I. Shklovskii, B. Shapiro, B. R. Sears, P. Lambrianides, and H. B. Shore, Statistics of spectra of disordered systems near the metal-insulator transition, Phys. Rev. B **47**, 11487 (1993).
[76] T. Guhr, A. Mueller-Gröeling, and H. A. Weidenmüller, Random matrix theories in quantum physics: Common concepts, Phys. Rep. **299**, 189 (1998).
[77] V. Oganesyan and D. A. Huse, Localization of interacting fermions at high temperature, Phys. Rev. B **75**, 155111 (2007).
[78] Y. Wang, H. Hu, and S. Chen, Many-body ground state localization and coexistence of localized and extended states in an interacting quasiperiodic system, Eur. Phys. J. B **89**, 77 (2016).
[79] Y. Wang, Y. Wang, and S. Chen, Spectral statistics, finite-size scaling and multifractal analysis of quasiperiodic chain with p-wave pairing, Eur. Phys. J. B **89**, 254 (2016).
[80] I. Y. Goldsheid and B. A. Khoruzhenko, Distribution of Eigenvalues in Non-Hermitian Anderson Models, Phys. Rev. Lett. **80**, 2897 (1998).
[81] L. G. Molinari, Non-Hermitian spectra and Anderson localization, J. Phys. A: Math. Theor. **42**, 265204 (2009).
[82] H. Markum, R. Pullirsch, and T. Wettig, Non-Hermitian Random Matrix Theory and Lattice QCD with Chemical Potential, Phys. Rev. Lett. **83**, 484 (1999).
[83] J. T. Chalker and B. Mehlig, Eigenvector Statistics in Non-Hermitian Random Matrix Ensembles, Phys. Rev. Lett. **81**, 3367 (1998)
[84] H. T. Quan, Z. Song, X. F. Liu, P. Zanardi, and C. P. Sun, Decay of Loschmidt Echo Enhanced by Quantum Criticality, Phys. Rev. Lett. **96**, 140604 (2006).
[85] M. Heyl, A. Polkovnikov, and S. Kehrein, Dynamical Quantum Phase Transitions in the Transverse-Field Ising Model, Phys. Rev. Lett. **110**, 135704 (2013).
[86] A. A. Zvyagin, Dynamical quantum phase transitions, Fiz. Nizk. Temp. (Kiev) **42**, 1240 (2016); Low Temp. Phys. **42**, 971 (2016).
[87] M. Heyl, Dynamical quantum phase transitions: A review, Rep. Prog. Phys. **81**, 054001 (2018).
[88] L. W. Zhou, Q.-H. Wang, H. L. Wang, and J. B. Gong, Dynamical quantum phase transitions in non-Hermitian lattices, Phys. Rev. A **98**, 022129 (2018).
[89] C. Yang, Y. Wang, P. Wang, X. Gao, and S. Chen, Dynamical signature of localization-delocalization transition in a one-dimensional incommensurate lattice, Phys. Rev. B **95**, 184201 (2017).
[90] Z. H. Xu, H. Huangfu, Y. B. Zhang, and S. Chen, Dynamical observation of mobility edges in one-dimensional incommensurate optical lattices, New J. Phys. **22**, 013036 (2020).
[91] M. Znojil, Non-Hermitian interaction representation and its use in relativistic quantum mechanics, Ann. Phys. (NY) **385**, 162 (2017).
[92] D. Krejcirik, P. Siegl, M. Tater, and J. Viola, Pseudospectra in non-Hermitian quantum mechanics, J. Math. Phys. **56**, 103513 (2015).